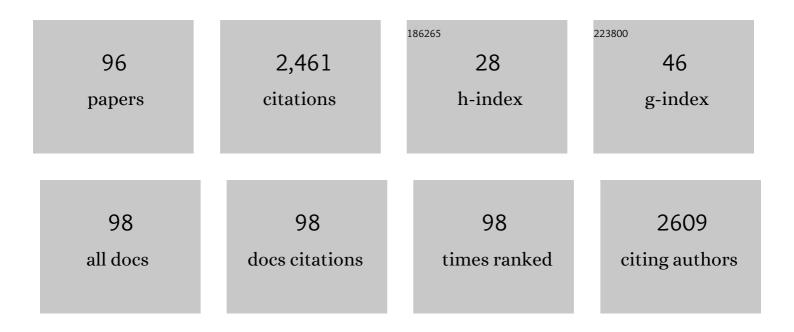
List of Publications by Year in descending order

Source: https://exaly.com/author-pdf/842232/publications.pdf Version: 2024-02-01



XINVIN LI

#	Article	IF	CITATIONS
1	Organic carbon remineralization rate in global marine sediments: A review. Regional Studies in Marine Science, 2022, 49, 102112.	0.7	5
2	The hadal zone is an important and heterogeneous sink of black carbon in the ocean. Communications Earth & Environment, 2022, 3, .	6.8	14
3	<i>In Situ</i> TEM Technique Revealing the Deactivation Mechanism of Bimetallic Pd–Ag Nanoparticles in Hydrogen Sensors. Nano Letters, 2022, 22, 3157-3164.	9.1	22
4	Chip-Based MEMS Platform for Thermogravimetric/Differential Thermal Analysis (TG/DTA) Joint Characterization of Materials. Micromachines, 2022, 13, 445.	2.9	4
5	Human Impacts Overwhelmed Hydroclimate Control of Soil Erosion in China 5,000ÂYears Ago. Geophysical Research Letters, 2022, 49, .	4.0	6
6	Area-Selective, In-Situ Growth of Pd-Modified ZnO Nanowires on MEMS Hydrogen Sensors. Nanomaterials, 2022, 12, 1001.	4.1	12
7	Microreactor-Based TG–TEM Synchronous Analysis. Analytical Chemistry, 2022, 94, 9009-9017.	6.5	6
8	Thermogravimetric Analysis on a Resonant Microcantilever. Analytical Chemistry, 2022, 94, 9380-9388.	6.5	16
9	Workâ€related helping and family functioning: A work–home resources perspective. Journal of Occupational and Organizational Psychology, 2021, 94, 55-79.	4.5	19
10	A discrete-time self-clocking complex electromechanical Æ©î"M gyroscope with quadrature error cancellation. Sensors and Actuators A: Physical, 2021, 317, 112470.	4.1	2
11	Thermodynamic Phase-like Transition Effect of Molecular Self-assembly. Journal of Physical Chemistry Letters, 2021, 12, 126-131.	4.6	4
12	Anatase porous titania nanosheets for resonant-gravimetric detection of ppb-level NO <sub>2</sub> at room-temperature. Analyst, The, 2021, 146, 4042-4048.	3.5	4
13	An Anti-Aliasing and Self-Clocking ΣΔM Cobweb-Like Disk Resonant MEMS Gyroscope with Extended Input Range. , 2021, , .		4
14	Nano beta zeolites catalytic-cracking effect on hydrochlorofluorocarbon molecule for specific detection of Freon. Journal of Materials Chemistry A, 2021, 9, 15321-15328.	10.3	8
15	Silicon-chip based electromagnetic vibration energy harvesters fabricated using wafer-level micro-casting technique. Journal of Micromechanics and Microengineering, 2021, 31, 035009.	2.6	2
16	Quantitative Structure–Activity Relationship of Nanowire Adsorption to SO <sub>2</sub> Revealed by <i>In Situ</i> TEM Technique. Nano Letters, 2021, 21, 1679-1687.	9.1	26
17	High-Aspect-Ratio TSV Process With Thermomigration Refilling of Au–Si Eutectic Alloy. IEEE Transactions on Components, Packaging and Manufacturing Technology, 2021, 11, 191-199.	2.5	4
18	Distribution, Source, and Burial of Sedimentary Organic Carbon in Kermadec and Atacama Trenches. Journal of Geophysical Research G: Biogeosciences, 2021, 126, e2020JG006189.	3.0	16

#	Article	IF	CITATIONS
19	Integrated Resonant Micro/Nano Gravimetric Sensors for Bio/Chemical Detection in Air and Liquid. Micromachines, 2021, 12, 645.	2.9	20
20	Three-Dimensional Arterial Pulse Signal Acquisition in Time Domain Using Flexible Pressure-Sensor Dense Arrays. Micromachines, 2021, 12, 569.	2.9	16
21	Ultra-Small Pixel IR Sensing Array Fabricated with a Post-CMOS Compatible Process. , 2021, , .		0
22	Porous Titania Nanosheets as Micro-Gravimetric Sensing Material for Trace NO2 Detection. , 2021, , .		0
23	Formaldehyde Sensor with Pentagram-Shaped Core-Shell Nanostructure as Catalyst. , 2021, , .		0
24	In-Plane Mode Encased Cantilevers for Cancer Cell Detection in Liquid. , 2021, , .		7
25	Computerized patterning method of Cliptronic jacquard structures. Textile Reseach Journal, 2021, 91, 3012-3022.	2.2	0
26	Silicon monolithic microflow sensors: a review. Journal of Micromechanics and Microengineering, 2021, 31, 104002.	2.6	2
27	Intelligent Modeling and Design of a Novel Temperature Control System for a Cantilever-Based Gas-Sensitive Material Analyzer. IEEE Access, 2021, 9, 21132-21148.	4.2	5
28	A spacer fabric-based three-dimensional patterning method with two-colored jacquard systems. Textile Reseach Journal, 2021, 91, 1399-1408.	2.2	1
29	100-μm-Scale High-Detectivity Infrared Detector With Thermopile/Absorber Double-Deck Structure Formed in (111) Silicon. IEEE Transactions on Electron Devices, 2021, , 1-7.	3.0	1
30	Happy But Uncivil? Examining When and Why Positive Affect Leads to Incivility. Journal of Business Ethics, 2020, 165, 595-614.	6.0	14
31	Dual-Resonator MEMS Magnetometer Based on Self-Clocking Sigma-Delta Modulation. IEEE Sensors Journal, 2020, 20, 1527-1535.	4.7	6
32	Through-Glass-Via Based Microstrip Band-Pass Filters Fabricated with Wafer-Level Low-Melting-Point Alloy Micro-Casting. IEEE Electron Device Letters, 2020, , 1-1.	3.9	12
33	An in-situ TEM microreactor for real-time nanomorphology & physicochemical parameters interrelated characterization. Nano Today, 2020, 35, 100932.	11.9	20
34	Generic Approach to Boost the Sensitivity of Metal Oxide Sensors by Decoupling the Surface Charge Exchange and Resistance Reading Process. ACS Applied Materials & Interfaces, 2020, 12, 37295-37304.	8.0	19
35	CMOS Compatible TSV Process with Post-CMOS Thermomigration Refilling of Au-Si Eutectic Alloy. , 2020, , .		1
36	Resonant-Cantilever-Detected Kinetic/Thermodynamic Parameters for Aptamer–Ligand Binding on a Liquid–Solid Interface. Analytical Chemistry, 2020, 92, 11127-11134.	6.5	2

#	Article	IF	CITATIONS
37	The catalytic-induced sensing effect of triangular CeO <sub>2</sub> nanoflakes for enhanced BTEX vapor detection with conventional ZnO gas sensors. Journal of Materials Chemistry A, 2020, 8, 11188-11194.	10.3	63
38	A Front-Side Microfabricated Thermoresistive Gas Flow Sensor for High-Performance, Low-Cost and High-Yield Volume Production. Micromachines, 2020, 11, 205.	2.9	3
39	Ultra-small pressure sensors fabricated using a scar-free microhole inter-etch and sealing (MIS) process. Journal of Micromechanics and Microengineering, 2020, 30, 065012.	2.6	14
40	Highly Sensitive p <sup>+</sup> Si/Al Thermopile-Based Gas Flow Sensors by Using Front-Sided Bulk Micromachining Technology. IEEE Transactions on Electron Devices, 2020, 67, 1781-1786.	3.0	8
41	Pentagram-Shaped Ag@Pt Core–Shell Nanostructures as High-Performance Catalysts for Formaldehyde Detection. ACS Applied Materials & Interfaces, 2020, 12, 8091-8097.	8.0	47
42	Detection of Phenylketonuria Markers Using a ZIF-67 Encapsulated PtPd Alloy Nanoparticle (PtPd@ZIF-67)-Based Disposable Electrochemical Microsensor. ACS Applied Materials & Interfaces, 2019, 11, 20734-20742.	8.0	43
43	Schiff-base reaction induced selective sensing of trace dopamine based on a Pt41Rh59 alloy/ZIF-90 nanocomposite. Nanotechnology, 2019, 30, 335708.	2.6	9
44	Modeling and realization for appearance visualization of Textronic laces. Textile Reseach Journal, 2019, 89, 4526-4536.	2.2	3
45	<i>In situ</i> construction of metal–organic framework (MOF) UiO-66 film on Parylene-patterned resonant microcantilever for trace organophosphorus molecules detection. Analyst, The, 2019, 144, 3729-3735.	3.5	50
46	A Front-Side Microfabricated Tiny-Size Thermopile Infrared Detector With High Sensitivity and Fast Response. IEEE Transactions on Electron Devices, 2019, 66, 2230-2237.	3.0	28
47	Enhancing the closed-loop stability of a high-Q polysilicon micro-hemispherical resonating gyroscope. AIP Advances, 2019, 9, .	1.3	3
48	Single-Side Fabricated p <sup>+</sup> Si/Al Thermopile-Based Gas Flow Sensor for IC-Foundry-Compatible, High-Yield, and Low-Cost Volume Manufacturing. IEEE Transactions on Electron Devices, 2019, 66, 821-824.	3.0	10
49	Schadenfreude: A Counternormative Observer Response to Workplace Mistreatment. Academy of Management Review, 2019, 44, 360-376.	11.7	50
50	An integrated micro-chip with Ru/Al2O3/ZnO as sensing material for SO2 detection. Sensors and Actuators B: Chemical, 2018, 262, 26-34.	7.8	64
51	A resonant cantilever based particle sensor with particle-size selection function. Journal of Micromechanics and Microengineering, 2018, 28, 085019.	2.6	15
52	Sub- <i>g</i> weak-vibration-triggered high-efficiency energy harvesting for event identification. Journal of Micromechanics and Microengineering, 2018, 28, 075018.	2.6	5
53	High-performance H2 sensors with selectively hydrophobic micro-plate for self-aligned upload of Pd nanodots modified mesoporous In2O3 sensing-material. Sensors and Actuators B: Chemical, 2018, 267, 83-92.	7.8	55
54	A Single-Side Fabricated Triaxis (111)-Silicon Microaccelerometer With Electromechanical Sigma–Delta Modulation. IEEE Sensors Journal, 2018, 18, 1859-1869.	4.7	16

#	Article	IF	CITATIONS
55	Design of a Dual Quantization Electromechanical Sigma–Delta Modulator MEMS Vibratory Wheel Gyroscope. Journal of Microelectromechanical Systems, 2018, 27, 218-230.	2.5	21
56	Ni-MOF-74 as sensing material for resonant-gravimetric detection of ppb-level CO. Sensors and Actuators B: Chemical, 2018, 262, 562-569.	7.8	42
57	An inconvenient truth? Interpersonal and career consequences of "maybe baby―expectations. Journal of Vocational Behavior, 2018, 104, 44-58.	3.4	38
58	Pt Nanoparticles Sensitized Ordered Mesoporous WO <sub>3</sub> Semiconductor: Gas Sensing Performance and Mechanism Study. Advanced Functional Materials, 2018, 28, 1705268.	14.9	231
59	Why and when job insecurity breeds abusive supervision. Proceedings - Academy of Management, 2018, 2018, 13198.	0.1	1
60	Predictors of parental leave support: Bad news for (big) dads and a policy for equality. Group Processes and Intergroup Relations, 2018, 21, 810-830.	3.9	5
61	Self-clocked dual-resonator micromachined Lorentz force magnetometer based on electromechanical sigma-delta modulation. , 2018, , .		6
62	Metal organic framework of MOF-5 with hierarchical nanopores as micro-gravimetric sensing material for aniline detection. Sensors and Actuators B: Chemical, 2018, 256, 639-647.	7.8	67
63	High-Performance Low-Range Differential Pressure Sensors Formed With a Thin-Film Under Bulk Micromachining Technology. Journal of Microelectromechanical Systems, 2017, 26, 879-885.	2.5	23
64	Resonant-Gravimetric Identification of Competitive Adsorption of Environmental Molecules. Analytical Chemistry, 2017, 89, 7031-7037.	6.5	20
65	Sources and compositional distribution of organic carbon in surface sediments from the lower Pearl River to the coastal South China Sea. Journal of Geophysical Research G: Biogeosciences, 2017, 122, 2104-2117.	3.0	28
66	Ni2(dobdc) MOF (metal-organic framework) nanocrystals for ultra-sensitive detection of ppb-level co with resonant-cantilever. , 2017, , .		0
67	ZnO-nanowire size effect induced ultra-high sensing response to ppb-level H2S. Sensors and Actuators B: Chemical, 2017, 240, 264-272.	7.8	93
68	Metal–Organic Frameworks for Resonant-Gravimetric Detection of Trace-Level Xylene Molecules. Analytical Chemistry, 2016, 88, 12234-12240.	6.5	59
69	A dual quantization electromechanical sigma-delta modulator vibratory wheel gyroscope. , 2016, , .		8
70	Microgravimetric Analysis Method for Activation-Energy Extraction from Trace-Amount Molecule Adsorption. Analytical Chemistry, 2016, 88, 4903-4908.	6.5	10
71	Amphiphilic Block Copolymer Templated Synthesis of Mesoporous Indium Oxides with Nanosheet-Assembled Pore Walls. Chemistry of Materials, 2016, 28, 7997-8005.	6.7	74
	Electromechanical Sigma–Delta Modulators ( <inline-formula> <tex-math) 0="" etqq0="" overlock<="" rgbt="" td="" tj=""><td>10 Tf 50 7</td><td>72 Td (notatio</td></tex-math)></inline-formula>	10 Tf 50 7	72 Td (notatio
72	Feedback Interfaces for Capacitive MEMS Inertial Sensors: A Review. IEEE Sensors Journal, 2016, 16, 6476-6495.	4.7	73

#	Article	IF	CITATIONS
73	A Tri-Beam Dog-Bone Resonant Sensor With High- in Liquid for Disposable Test-Strip Detection of Analyte Droplet. Journal of Microelectromechanical Systems, 2016, 25, 244-251.	2.5	11
74	μ-â€~Diving suit' for liquid-phase high-Q resonant detection. Lab on A Chip, 2016, 16, 902-910.	6.0	11
75	Polydopamine nanotubes: bio-inspired synthesis, formaldehyde sensing properties and thermodynamic investigation. Journal of Materials Chemistry A, 2016, 4, 3487-3493.	10.3	99
76	Single-Side Fabrication of Multilevel 3-D Microstructures for Monolithic Dual Sensors. Journal of Microelectromechanical Systems, 2015, 24, 531-533.	2.5	10
77	Synergistic improvement of gas sensing performance by micro-gravimetrically extracted kinetic/thermodynamic parameters. Analytica Chimica Acta, 2015, 863, 49-58.	5.4	9
78	Length-extensional resonating gas sensors with IC-foundry compatible low-cost fabrication in non-SOI single-wafer. Microelectronic Engineering, 2015, 136, 1-7.	2.4	15
79	Regioselective Patterning of Multiple SAMs and Applications in Surface-Guided Smart Microfluidics. ACS Applied Materials & Interfaces, 2014, 6, 21961-21969.	8.0	20
80	Microgravimetric Thermodynamic Modeling for Optimization of Chemical Sensing Nanomaterials. Analytical Chemistry, 2014, 86, 4178-4187.	6.5	66
81	Mesoporous Silica Nanoparticles (MSNs) for Detoxification of Hazardous Organophorous Chemicals. Small, 2014, 10, 2404-2412.	10.0	41
82	Package-friendly piezoresistive pressure sensors with on-chip integrated packaging-stress-suppressed suspension (PS <sup>3</sup> ) technology. Journal of Micromechanics and Microengineering, 2013, 23, 045027.	2.6	32
83	In situ growth of noble metal nanoparticles on graphene oxide sheets and direct construction of functionalized porous-layered structure on gravimetric microsensors for chemical detection. Chemical Communications, 2012, 48, 10784.	4.1	40
84	Hyper-branched sensing polymer directly constructed on a resonant micro-cantilever for the detection of trace chemical vapor. Journal of Materials Chemistry, 2012, 22, 18004.	6.7	32
85	Integrated microcantilevers for high-resolution sensing and probing. Measurement Science and Technology, 2012, 23, 022001.	2.6	48
86	Fully front-side bulk-micromachined single-chip micro flow sensors for bare-chip <i>SMT</i> (surface) Tj ETQq0 0	0 rgBT /Ov	verlock 10 Tf
87	Three Dimensional PtRh Alloy Porous Nanostructures: Tuning the Atomic Composition and Controlling the Morphology for the Application of Direct Methanol Fuel Cells. Advanced Functional Materials, 2012, 22, 3570-3575.	14.9	103
88	A chelating-bond breaking and re-linking technique for rapid re-immobilization of immune micro-sensors. Biomedical Microdevices, 2012, 14, 303-311.	2.8	9
89	Monolithic Integration of Pressure Plus Acceleration Composite TPMS Sensors With a Single-Sided Micromachining Technology. Journal of Microelectromechanical Systems, 2012, 21, 284-293.	2.5	49
90	Functionalized Mesoporous Silica for Microgravimetric Sensing of Trace Chemical Vapors. Analytical	6.5	111

111 6.5

Chemistry, 2011, 83, 3448-3454.

#	Article	IF	CITATIONS
91	Single-Side Fabricated Pressure Sensors for IC-Foundry-Compatible, High-Yield, and Low-Cost Volume Production. IEEE Electron Device Letters, 2011, 32, 979-981.	3.9	38
92	A High-Performance Dual-Cantilever High-Shock Accelerometer Single-Sided Micromachined in (111) Silicon Wafers. Journal of Microelectromechanical Systems, 2010, 19, 1515-1520.	2.5	36
93	Resonant-cantilever bio/chemical sensors with an integrated heater for both resonance exciting optimization and sensing repeatability enhancement. Journal of Micromechanics and Microengineering, 2009, 19, 045023.	2.6	70
94	Nanofabrication based on MEMS technology. IEEE Sensors Journal, 2006, 6, 686-690.	4.7	13
95	Single-side micromachined ultra-small thermopile IR detecting pixels for dense-array integration. Journal of Micromechanics and Microengineering, 0, , .	2.6	0
96	CO <sub>2</sub> sensing properties and mechanism of ZnMn <sub>2</sub> O <sub>4</sub> nanotubes under air and inert conditions. Journal of Materials Chemistry C, 0, , .	5.5	0